

show any absorption features in the wavelength range 0.80–3  $\mu\text{m}$ . The resonance peak in the  $\chi^{(3)}$  spectra of PPI and PMOPI was  $\sim 1.2$  and  $\sim 1.35$   $\mu\text{m}$ , respectively, and hence suggests a three-photon resonance as the origin of the observed peak in the wavelength dispersion of the third-order optical susceptibility. As shown in Table I, the magnitude of the three-photon resonance enhanced  $\chi^{(3)}$  of PPI and PMOPI was  $1.6 \times 10^{-11}$  and  $5.4 \times 10^{-11}$  esu, respectively. Thus, three-photon resonance enhancements result in about 1 order of magnitude increase for PPI and a factor of 8 increase for PMOPI above the nonresonant optical nonlinearities for these two aromatic poly(azomethines).

Although a detailed quantitative comparison of the measured third-order optical nonlinearities of PPI and PMOPI cannot be made with those of their isoelectronic vinylene polymers PPV and PDMOPV because the complete  $\chi^{(3)}$  spectrum of any of the vinylene polymers has not been reported, a qualitative comparison is in order. In the case of the Schiff base polymer PPI and its vinylene analogue PPV, the two polymers exhibit similar optical absorption spectra<sup>4</sup> with a  $\lambda_{\text{max}}$  at 405 nm. Therefore, a similar dispersion due to three-photon resonance can be expected in the  $\chi^{(3)}$  spectrum of PPV as observed in Figure 2 for PPI. The reported  $\chi^{(3)}(-3\omega; \omega, \omega, \omega)$  of PPV at 1.85  $\mu\text{m}$  ( $7.8 \times 10^{-12}$  esu) is most likely resonantly enhanced. For comparison purposes, the corresponding  $\chi^{(3)}$  value of PPI at 1.83  $\mu\text{m}$  is  $3.3 \times 10^{-12}$  esu and this value too is resonantly enhanced. In the case of PDMOPV, the reported  $\chi^{(3)}$  of  $5.4 \times 10^{-11}$  esu at 1.85  $\mu\text{m}$  is to be compared with  $1.5 \times 10^{-11}$  esu for PMOPI at 1.83  $\mu\text{m}$ . Here, the major difference in the optical nonlinearities of PMOPI and PDMOPV can be traced to two factors. First, it should be noticed that PDMOPV at 1.85  $\mu\text{m}$  is much closer to a three-photon resonance peak ( $\sim 1.5$   $\mu\text{m}$ ) than PMOPI is at 1.83  $\mu\text{m}$  to its three-photon resonance at 1.35  $\mu\text{m}$ . Second, the greater degree of  $\pi$ -electron delocalization in PDMOPV ( $\lambda_{\text{max}} = 500$  nm) compared to PMOPI ( $\lambda_{\text{max}} = 450$  nm) also contributes to the larger optical nonlinearity. The greater  $\pi$ -electron delocalization in PDMOPV is due to 2,5-dimethoxy substitution on every *p*-phenylene ring of the polymer, whereas only every other *p*-phenylene ring in PMOPI is so substituted. Thus, it can be anticipated that 2,5-dimethoxy substitution on every ring of PMOPI will further enhance the optical nonlinearity.

In summary, we have investigated the third-order nonlinear optical properties of two conjugated aromatic Schiff base polymers, PPI and PMOPI, by picosecond third harmonic generation and show that they are a new class of third-order nonlinear optical materials. The measured  $|\chi^{(3)}(-3\omega, \omega, \omega, \omega)|$  spectra of PPI and PMOPI in the wavelength range 0.9–2.4  $\mu\text{m}$  showed a three-photon resonance peak at 1.2 and 1.35  $\mu\text{m}$ , respectively. The resulting resonance enhanced  $\chi^{(3)}$  was  $1.6 \times 10^{-11}$  and  $5.4 \times 10^{-11}$  esu for PPI and PMOPI, respectively. The nonresonant  $|\chi^{(3)}|$  values of PPI and PMOPI at 2.4  $\mu\text{m}$  were  $1.6 \times 10^{-12}$  and  $7.3 \times 10^{-12}$  esu, respectively. These results show that a simple structural modification of PPI, as realized in its derivative PMOPI, results in a factor of 3–5 enhancement of the cubic nonlinear optical properties over the entire spectrum of  $\chi^{(3)}$  investigated. Furthermore, three-photon resonance evidenced in the dispersion of  $\chi^{(3)}$  enhanced the optical nonlinearities by about a factor of 10 above the off-resonance nonlinearities. Considering the many as-yet unexplored possible structural modifications afforded by the conjugated Schiff base polymers, it can be expected that larger  $\chi^{(3)}$  values may be found in other derivatives.

**Acknowledgment.** Work at the University of Roch-

ester was supported by the New York State Science and Technology Foundation, Amoco Foundation, and National Science Foundation (Grant CHE-881-0024). The nonlinear optical characterization was carried out at Du Pont. H.V. acknowledges the valuable technical assistance of J. Kelly.

**Registry No.** PPI (SRU), 28157-08-6; PMOPI (SRU), 135789-42-3.

## Comparison of Simultaneous and Preirradiation Grafting of Methyl Methacrylate onto a Porous Membrane

Hideyuki Yamagishi, Kyoichi Saito,\* and Shintaro Furusaki

Department of Chemical Engineering  
Faculty of Engineering, University of Tokyo  
Hongo, Tokyo 113, Japan

Takanobu Sugo and Isao Ishigaki

Japan Atomic Energy Research Institute  
Takasaki Radiation Chemistry  
Research Establishment  
Takasaki, Gunma 370-12, Japan

Received June 5, 1991

Revised Manuscript Received September 26, 1991

Radiation-induced graft polymerization is an effective technique for tailoring existing polymers of various shapes. We adopted porous membranes in a flat sheet<sup>1</sup> or hollow fiber<sup>2</sup> as a trunk polymer and introduced the chelate-forming groups<sup>3</sup> and affinity ligands.<sup>4</sup> Radiation-induced grafting can be classified into two categories: (1) simultaneous irradiation or preirradiation grafting; (2) vapor-phase or liquid-phase grafting. In addition, the preirradiation technique can be divided into two modes: with or without exposure to air before grafting. In a previous paper,<sup>5</sup> porous cellulose triacetate membrane was irradiated in a nitrogen atmosphere, and after exposure to air for about 1 min, methyl methacrylate (MMA) was contacted with the membrane in vapor and liquid phases, and the water permeability of the resulting MMA-grafted membranes was then compared. When the trunk polymer had a porous structure, the grafted polymer branches were formed both on the surface of the internal macropore and in the amorphous domain of the polymer matrix. To control the water permeability of the porous functional membrane, it is important to select the grafting technique governing the location of the grafted polymer branches. We report here the comparison of the water permeability of the MMA-grafted membranes prepared by the two modes of vapor-phase grafting and discuss the location of the grafted polymer branches.

A commercially available porous cellulose triacetate (CTA) membrane (FM22, Fuji Film Co., Ltd., Japan) was used as the trunk polymer for grafting. The diameter and

(1) Saito, K.; Hori, T.; Furusaki, S.; Sugo, T.; Okamoto, J. *Ind. Eng. Chem. Res.* 1987, 26, 1977.

(2) Saito, K.; Uezu, K.; Hori, T.; Furusaki, S.; Sugo, T.; Okamoto, J. *AIChE J.* 1988, 34, 411.

(3) Saito, K.; Kaga, T.; Yamagishi, H.; Furusaki, S.; Sugo, T.; Okamoto, J. *J. Membr. Sci.* 1989, 43, 131.

(4) Kim, M.; Saito, K.; Furusaki, S.; Sugo, T.; Ishigaki, I. *J. Chromatogr.* 1991, 585, 45.

(5) Yamagishi, H.; Saito, K.; Furusaki, S.; Sugo, T.; Okamoto, J. *Chem. Mater.* 1990, 2, 705.

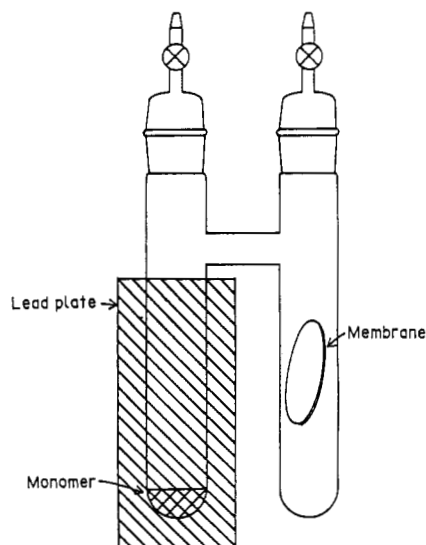


**Figure 1.** Reaction ampule for vapor-phase grafting without exposure to air.

thickness of the membrane were 47.4 and 0.179 mm, respectively, in a wet state. The membrane has a nominal 0.22- $\mu\text{m}$ -diameter pore size and 70% porosity. MMA-grafted membranes were prepared by two modes of radiation-induced graft polymerization: simultaneous irradiation and preirradiation. Figure 1 shows an H-shaped glass ampule for vapor-phase grafting. Use of the H-shaped ampule enabled us to contact the membrane with vapor of the monomer without exposure to air. In contrast, in our previous study,<sup>5</sup> the irradiated trunk polymer was exposed to air for the sake of experimental convenience. One leg of the H-shaped ampule contained 3 mL of MMA as the monomer, and the other leg contained a porous CTA membrane as the trunk polymer. The MMA-containing leg was shielded completely with a lead plate to prevent formation of a homopolymer by irradiation.

For the simultaneous-irradiation grafting technique, both legs were filled with MMA vapor, and the CTA membrane was irradiated by  $^{60}\text{Co}$   $\gamma$  rays to initiate graft polymerization. The CTA membrane was taken out of the reaction ampule after a predetermined period ranging from 30 to 90 min. The graft polymerization was carried out at ambient temperature. The total dose for a 90-min reaction was 1.2 kGy. For the preirradiation grafting technique, the MMA liquid was frozen, and the ampule was then evacuated. Irradiation of the electron beam onto the porous CTA membrane was performed at ambient temperature by means of a cascade electron accelerator (Dynamitron, IEA-3000-25-2, Radiation Dynamics Co.) operated at a voltage of 2.0 MeV and current of 1 mA. The total dose was set to 200 kGy. After irradiation, MMA was thawed, and its vapor diffused into the membrane to initiate graft polymerization. The reaction temperature was 313 K. The reaction time ranged up to 30 min.

The homopolymer in the resulting membrane was removed with benzene. The MMA-grafted membrane was dried under reduced pressure and its weight was measured. The degree of grafting ( $d_g$ ), defined in eq 1, ranged from 10 to 100%:

$$d_g = [(W_1 - W_0)/W_0]100 \quad (1)$$

where  $W_0$  and  $W_1$  are the weights of the starting and MMA-grafted membranes, respectively. The MMA-grafted membranes prepared by simultaneous irradiation and preirradiation grafting will hereafter be referred to as S-MMA-CTA and P-MMA-CTA membranes, respectively.

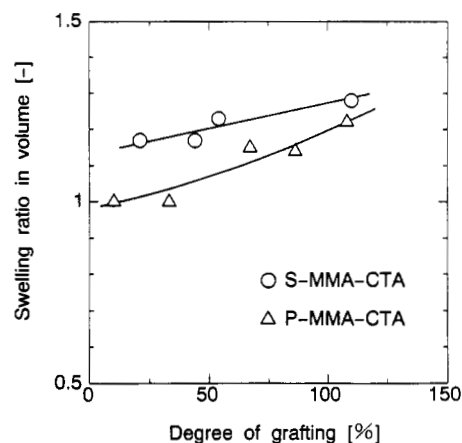


**Figure 2.** Swelling ratio in volume vs degree of grafting.

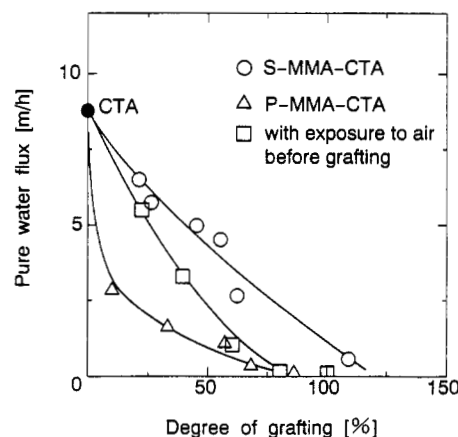


**Figure 3.** Pure water flux vs degree of grafting.

The diameter and thickness of the resulting membranes were measured with a scale and a thickness meter in a wet state. The swelling ratio in volume as a function of the degree of grafting is compared between the S-MMA-CTA and P-MMA-CTA membranes in Figure 2. Here, the swelling ratio is defined as the volume ratio of the MMA-grafted membrane to the starting membrane. The S-MMA-CTA membrane swelled more than the P-MMA-CTA membrane.

The experimental apparatus and procedures for measuring the water permeability of the MMA-grafted membrane were described in our previous paper.<sup>5</sup> The flow rate of pure water permeating across the porous membrane at a filtration pressure of about  $1.0 \times 10^5$  Pa was converted into the pure water flux (PWF) by dividing by the membrane surface area. The S-MMA-CTA membrane exhibited a higher PWF than the P-MMA-CTA membrane with the same amount of grafted polymer branches, i.e., the same degree of grafting, as shown in Figure 3. For instance, the PWF of the S-MMA-CTA membrane was 4 times larger than that of the P-MMA-CTA membrane with the same  $d_g$ , 50%. For comparison, the PWF of the membrane which was prepared by the preirradiation technique with exposure to air before grafting is also plotted as a function of the degree of grafting in Figure 3. The relationship was intermediate between those of S-MMA-CTA and P-MMA-CTA membranes.

From the above results, we can discuss the location of the polymer branches grafted onto the porous membrane according to three modes of radiation-induced grafting techniques. Irradiation of an electron beam or  $\gamma$ -rays can induce the uniform formation of radicals throughout the trunk polymer consisting of the macropore and polymer

matrix. The polymer branches may be distributed both on the surface of the internal macropore and in the amorphous domain of the polymer matrix. The distribution ratio causes the difference in the water permeability of the monomer-grafted membrane. For simultaneous irradiation grafting, a higher amount of the polymer branches is grafted in the polymer matrix because the radical reacts with monomer previously penetrated in the polymer matrix before irradiation. In contrast, for pre-irradiation grafting, the monomer needs to be diffused into the polymer matrix toward the radical after irradiation, and thus a higher amount of the polymer branches is grafted on the surface of the internal macropore. When the irradiated membrane is exposed to air before grafting, the radical on the surface of the internal macropore decays instantaneously because of the oxygen diffusion. Therefore, the monomer will invade the polymer matrix more deeply compared to the preirradiation grafting without exposure to air. A higher amount of the polymer branches in the polymer matrix than on the surface of the internal macropore results in a higher swelling ratio and PWF of the monomer-grafted membrane.

In summary, we have found that we can control the location of the polymer branches grafted onto the porous material by selecting not only the combination of trunk polymer and monomer but also the grafting technique, such as simultaneous/preirradiation grafting with/without exposure to air. This principle may be of interest for modifying existing porous materials into the functional porous materials by radiation-induced graft polymerization.

## Photochemical Preparation of Crystalline Silicon Nanoclusters

J. M. Jasinski\* and F. K. LeGoues

IBM Research Division  
Thomas J. Watson Research Center  
Yorktown Heights, New York 10598

Received July 11, 1991

Revised Manuscript Received August 29, 1991

There is considerable current interest in the preparation and properties of nanometer-size semiconductor crystallites.<sup>1</sup> Such nanoclusters exhibit novel materials properties largely as a consequence of their finite small size. Most of the existing work on semiconductor nanoclusters has concentrated on II-VI, IV-VI, and III-V materials such as CdS, PbS, and GaAs. There have been very few reports of the preparation of group IV nanoclusters. Some results are available for Ge nanoclusters prepared by gas evaporation methods<sup>2</sup> and for Ge nanoclusters isolated in SiO<sub>2</sub> which are prepared by cosputtering.<sup>3</sup> In addition, quantum size effects have been attributed to microcrystalline silicon films and silicon nanoparticles prepared by slow discharge methods.<sup>4</sup> Intriguing results, such as

tunable visible photoluminescence, have also been reported for electrochemically etched samples of silicon, with the effects being attributed to the formation of quantum wires in the material.<sup>5</sup>

A difficulty in the preparation of discrete group IV nanoclusters, compared to the preparation of compound semiconductor materials, is an apparent lack of synthetic chemical methods for their preparation. In this paper we report the unexpected finding that silicon nanoclusters can be formed in the gas-phase, room-temperature photolysis of disilane with the output from an ArF excimer laser operating at 193 nm. This observation may lead ultimately to the preparation of useful macroscopic quantities of these materials for further study and possible applications in silicon-based optoelectronics and nonlinear optics.

Photolysis of disilane has been used by various groups over the past 10 years to deposit silicon films ranging in crystallinity from amorphous hydrogenated silicon to epitaxial silicon.<sup>6</sup> Several studies of the photochemistry of disilane at 193 nm have also been carried out.<sup>7-10</sup> The photodissociation process is exceedingly complicated, with numerous possible product channels and the generation of numerous possible silicon hydride reactive intermediates. There have also been reports of the formation of hydrogenated amorphous silicon powder under various photolysis conditions.<sup>11,12</sup> This process is normally viewed as detrimental to thin-film deposition. By exercising some control over the photolysis conditions, we find that we can turn the "nuisance" of gas-phase powder formation into a potentially useful synthetic pathway for the formation of silicon nanoclusters.

Samples were prepared by the photolysis of disilane dilute in helium buffer gas in a stainless steel flow cell which is identical in all important aspects to those we have previously described in studies of the spectroscopy and kinetics of silicon hydride reactive intermediates.<sup>13</sup> The cell was evacuated with an mechanical pump and was operated under conditions of constant total flow and constant total pressure. The base pressure of the system was in the milliTorr range. The total flow was 100 sccm and the total pressure was 5 Torr in all experiments. The disilane partial pressure was varied from 0 to 200 mTorr. From the measured leak/outgassing rate of the cell, we estimate that the partial pressure of oxygen, water, and hydrocarbons was in the 10<sup>-4</sup>-Torr range during depositions. The higher quality samples (smallest crystallites) were typically deposited with a disilane partial pressure of 15-25 mTorr. The photolysis source was the unfocused output of an ArF excimer laser operating at 193 nm. The laser beam entered the cell through a helium-purged Su-

(4) Furukawa, S.; Miyasato, T. *Phys. Rev. B* 1988, 38, 5726. Takagi, H.; Ogawa, H.; Yamazaki, Y.; Ishizaki, A.; Nakagiri, T. *Appl. Phys. Lett.* 1990, 56, 2379.

(5) Canham, L. T. *Appl. Phys. Lett.* 1990, 57, 1046.

(6) See, for example: Mishima, Y.; Hirose, M.; Osaka, Y.; Nagamine, K.; Ashida, Y.; Kitagawa, N.; Isogaya, K. *Jpn. J. Appl. Phys. Lett.* 1983, 22, L46. Yoshikawa, A.; Yamaga, S. *Jpn. J. Appl. Phys. Lett.* 1984, 23, L91. Lian, S.; Fowler, B.; Bullock, D.; Banerjee, S. *Appl. Phys. Lett.* 1991, 58, 514.

(7) Stafast, H. *Appl. Phys. A* 1988, 45, 93.

(8) Chu, J. O.; Begemann, M. H.; McKillop, J. S.; Jasinski, J. M. *Chem. Phys. Lett.* 1989, 155, 576. Jasinski, J. M. *Chem. Phys. Lett.*, 1991, 183, 558.

(9) Eres, D.; Geohegan, D. B.; Lowndes, D. H.; Mashburn, D. N. *Appl. Surf. Sci.* 1989, 36, 70.

(10) Muranaka, Y.; Motooka, T.; Lubben, D.; Greene, J. E. *J. Appl. Phys.* 1989, 66, 910.

(11) Jasinski, J. M.; Chu, J. O.; Begemann, M. H. *Mater. Res. Soc. Symp. Proc.* 1989, 131, 487.

(12) Dietrich, T. R.; Chiussi, S.; Stafast, H.; Comes, F. J. *Appl. Phys. A* 1989, 48, 405.

(13) Jasinski, J. M. *J. Phys. Chem.* 1986, 90, 555. Jasinski, J. M.; Chu, J. O. *J. Chem. Phys.* 1988, 88, 1678.

(1) Bawendi, M.; Steigerwald, M. L.; Brus, L. E. *Annu. Rev. Phys. Chem.* 1990, 41, 477. Wang, Y.; Herron, N. J. *Phys. Chem.* 1991, 95, 525.

(2) Hayashi, S.; Wakayama, H.; Okada, T.; Kim, S. S.; Yamamoto, K. *J. Phys. Soc. Jpn.* 1987, 56, 243.

(3) Fujii, M.; Hayashi, S.; Yamamoto, K. *Jpn. J. Appl. Phys.* 1991, 30, 687. Hayashi, S.; Fujii, M.; Yamamoto, K. *Jpn. J. Appl. Phys. Lett.* 1989, 28, L1464. Fujii, M.; Hayashi, S.; Yamamoto, K. *Appl. Phys. Lett.* 1990, 57, 2692.